J. Physiol. (1987), **386**, *pp.* 547–570
With 18 text-figures
Printed in Great Britain

KINETICS AND SELECTIVITY OF A LOW-VOLTAGE-ACTIVATED CALCIUM CURRENT IN CHICK AND RAT SENSORY NEURONES

BY E. CARBONE* AND H. D. LUX

From the Department of Neurophysiology, Max Planck Institute for Psychiatry, D-8033 Planegg, F.R.G.

(*Received 25 April 1986*)

SUMMARY

1. Using the whole-cell recording mode of the patch-clamp technique, we have investigated kinetic and selectivity properties of a low-voltage-activated (l.v.a.) Ca^{2+} current in chick and rat dorsal root ganglion (d.r.g.) neurones.

2. L.v.a currents were activated at about −50 mV and reached maximum amplitudes between −30 and −20 mV with averages of −0·16 nA in chick and −0·3 nA in rat d.r.g. cells with 5 mM-extracellular Ca^{2+}. Between −60 and −20 mV, the time to peak, t_p, of this current decreased with increasing membrane depolarizations. An e-fold change of t_p required a 14 mV potential change in chick and a 17 mV change in rat d.r.g. cells at 22 °C.

3. Between −50 and +20 mV inactivation of this current was fast, single exponential and voltage dependent. In rat, the time constant of inactivation, τ_h, was smaller and less voltage dependent than in chick.

4. The amplitude of these currents increased by a factor of 5–10, when the extracellular Ca^{2+} concentration was changed from 1 to 95 mM. Amplitudes and kinetic parameters of the currents showed typical shifts along the voltage axis. No correlation between Ca^{2+} current amplitudes and activation–inactivation kinetics was found, suggesting that the reaction rates which control these processes are not dependent on Ca^{2+} entry.

5. Recovery from inactivation was voltage dependent and developed with a time constant, τ_r, in the order of 1 s. τ_r was nearly halved by changing the potential from −80 to −120 mV.

6. Tail currents associated with membrane repolarization were also voltage dependent and developed exponentially. Their time constant decreased by a factor of 3 when the potential was changed from −60 to −100 mV.

7. A second and more prominent Ca^{2+} current was activated at potentials positive to −20 mV (high-voltage-activated Ca^{2+} currents, h.v.a.), masking the time course of l.v.a. currents. Between −20 and 0 mV, time to peak of the entire current increased by a factor of 2 but decreased again at higher membrane potentials. Inactivation also became significantly slower in this potential range.

8. The contribution of the h.v.a. component to the total membrane current was

* Present address: Dipartimento di Anatomia e Fisiologia Umana, Sezione di Neuroscienze, Corso Raffaello 30, I-10125 Torino, Italy.

markedly reduced using a high intracellular Ca^{2+} concentration, $[Ca^{2+}]_i$, or internal fluoride salts. This made it possible to study the kinetic parameters and the I–V characteristics of the l.v.a. current more precisely over a wider potential range (−50 to +30 mV).

9. L.v.a. and h.v.a. currents were blocked reversibly by 5 mM-Ni^{2+} or 100 μM-Cd^{2+}. Replacement of Ca^{2+} with Ba^{2+} reduced the l.v.a. currents by about one-fifth, but roughly doubled the amplitude of h.v.a. currents. Sr^{2+}, on the other hand, increased the amplitude of both l.v.a. and h.v.a. components by one-fifth. Mg^{2+} currents through this channel could not be resolved.

INTRODUCTION

There is increasing evidence that neuronal membranes possess two types of Ca^{2+} channels (Llinás & Yarom, 1981; Llinás & Jahnsen, 1982; Murase & Randic, 1983). In vertebrate dorsal root ganglion neurones (Carbone & Lux, 1984*a*; Bossu, Feltz & Thomann, 1985; Fedulova, Kostyuk & Veselovsky, 1985; Nowycky, Fox & Tsien, 1985) and rat pituitary cells (Matteson & Armstrong, 1986; DeRiemer & Sakmann, 1986) the two types of Ca^{2+} channels show different ranges of voltage activation and different inactivation time courses. The low-voltage-activated (l.v.a.) channel turns on between −50 and −30 mV, inactivates faster and is rather insensitive to organic Ca^{2+}-antagonists (Boll & Lux, 1985). This channel is metabolically stable and remains functional in excised membrane patches for a long time (Carbone & Lux, 1984*b*). The high-voltage-activated (h.v.a.) channel turns on between −20 and 0 mV, is metabolically unstable (Fedulova *et al.* 1985) and inactivates slowly. This channel resembles the classical Ca^{2+} channel described in other preparations (see Hagiwara & Byerly, 1981, for a review). The latter has been also designated as the 'slow' (Fedulova *et al.* 1985), the 'L' (Nowycky *et al.* 1985) and the 'fast-deactivating' (Matteson & Armstrong, 1986) Ca^{2+} channel. Our l.v.a. channel is accordingly named 'fast', 'T' or 'slow deactivating'.

There are no detailed reports on kinetics and selectivity properties of the l.v.a. Ca^{2+} channel. This is needed since this channel has been implicated in the control of various cellular functions, such as: (1) modulation of the cyclical firing patterns of central mammalian neurones (Llinás & Yarom, 1981); (2) regulation of hormone secretion in endocrine cells (DeRiemer & Sakmann, 1986); (3) contraction of slow muscles in molluscs (Mackie & Meech, 1985); and (4) beating of the ciliary system in protozoa (Deitmer, 1984).

In the present paper, we have investigated in more detail the kinetic and selectivity properties of l.v.a. Ca^{2+} channels on the basis of whole-cell currents. Attention was given to three major points: (i) separation of l.v.a. from h.v.a. Ca^{2+} currents in order to study the kinetic parameters of l.v.a. channels over a wider range of membrane potentials than previously reported; (ii) an assessment of the properties of the inactivation gate; and (iii) a comparison of the ionic selectivity of l.v.a. and h.v.a. channels. We found that internal dialysis with fluoride salts or solutions with high internal free Ca^{2+} removed the h.v.a channel with little effect on the l.v.a. type, confirming previous results on snail neurones (Kostyuk & Krishtal, 1977). The l.v.a. channel so isolated appears to possess kinetic and selectivity properties distinctly

different from those of the classical Ca^{2+} channel. It inactivates in a voltage-dependent manner which does not appear to be influenced by the rate of Ca^{2+} entry. The l.v.a. channel conducts all alkaline earth ions equally well, except for Mg^{2+}.

METHODS

The experiments were performed on primary cultures of dorsal root ganglia (d.r.g.). Sensory neurones from the thoracic and lumbar region were dissociated from 10-day-old chick embryos (*Gallus domesticus*) or 19-day-old rat embryos and grown in culture according to the method of Barde, Edgar & Thoenen (1980). Dissociated cells were plated on 32 mm plastic Petri dishes and maintained at 37 °C in a CO_2 incubator. Patch-clamp measurements were performed at 23 °C, 6–12 h after plating.

Solutions

The compositions of the solutions used are listed in Table 1. All solutions were filtered through a 0·2 μm Millipore filter before use. External solutions were Na^+ and K^+ free, and contained 3×10^{-7} M-tetrodotoxin (TTX, Sigma, Munich, F.R.G.). To improve the quality of the patch conditions, the osmolarity of the pipette-filling solution was reduced by 20%. The level of free Ca^{2+} in the intracellular medium was calculated taking the following apparent stability constants for the Ca^{2+} buffers at pH 7·3: 1×10^{-7} M for the ethyleneglycol-bis(oxyethylenenitrile)tetraacetic acid (EGTA, Merck, Darmstadt), $2{\cdot}17 \times 10^{-6}$ M for *N'*-(2-hydroxyethyl)-ethylenediamine-*N*, *N*, *N'*-triacetate (HEDTA, Sigma, Munich) and $1{\cdot}18 \times 10^{-4}$ M for nitrilotriacetic-acid (NTA, Sigma, Munich) (Bjerrum, Schwarzenbach & Sillen, 1957; Martell & Smith, 1974). The Ca^{2+} antagonist Verapamil (Knoll, Ludwigshafen, F.R.G.) was used in some experiments. When F^- was used in internal solutions, CsCl was replaced with CsF.

Current measurements

Whole-cell clamp currents were measured according to the method of Hamill, Marty, Neher, Sakmann & Sigworth (1981). Pipettes were fabricated from thick-walled Duran glass (Schott Ruhrglas, Mainz, F.R.G.) and coated with Sylgard (Dow Corning, Seneffe, Belgium). They had resistances of about 3 MΩ when filled with standard pipette solutions (120 mM-Cs^+, see Table 1). Membrane currents were recorded using an *I–V* converter similar to that described elsewhere (Lux & Brown, 1984).

Voltage steps were delivered through a pulse generator operated manually. Membrane currents were stored on an FM tape-recorder at 5 kHz. Data were digitized off-line at sampling times of 50–150 μs using a 12-bit analog-to-digital converter in combination with an LSI 11/23 minicomputer. In some cases, however, stimulation and data acquisition was done on-line. Capacitative currents were reduced to nearly one-third of their size by an analog circuit during the experiment. The residual current artifacts were minimized by subtracting appropriately scaled responses to 40 mV hyperpolarizing pulses from the holding potential. Series resistance compensation for the pipette resistance (5–6 MΩ following establishment of whole-cell clamp) was used to obtain maximal response time constants of 20–40 μs. To avoid feed-back saturation, care was taken to record from cells in which Ca^{2+} currents did not exceed 1 nA. This also limited the error introduced by an uncompensated series resistance to 1–5 mV.

To achieve optimum conditions for whole-cell recording, all experiments were performed on freshly prepared cells (6–12 h after plating) (Carbone & Lux, 1986*a*). At this stage of growth, most d.r.g. cells are small (10–15 μm in diameter), round and lack processes. These three conditions allow appropriate voltage- and space-clamp control, as shown by the absence of notch-like discontinuities on the current traces at low membrane potentials (−40 and −10 mV). On the other hand, seal resistance of 50 GΩ could be easily obtained on these cells and access to the cell interior after breaking through the cell membrane was usually as satisfactory as evidenced by the large amplitude and small time constant of the decaying part of the capacitive artifact. The kinetic and selectivity properties of Ca^{2+} channels in these cells were found to be similar to those of mature cells (1–4 days). Mature cells were larger (20–40 μm) and possessed long processes which normally created space-clamp difficulties.

TABLE 1. Composition of solutions (mM)

External cations	Choline chloride	$CaCl_2$	$MgCl_2$	$NiCl_2$	$BaCl_2$	$SrCl_2$	HEPES*
1 Ca^{2+}	120	1	6	—	—	—	10
5 Ca^{2+}	120	5	2	—	—	—	10
20 Ca^{2+}	120	20	2	—	—	—	10
95 Ca^{2+}	—	95	—	—	—	—	10
5 Ni^{2+}	120	—	—	5	—	—	10
20 Ba^{2+}	120	—	2	—	20	—	10
20 Sr^{2+}	120	—	2	—	—	20	10

Internal cations	CsCl	NMGCl†	TEACl	$CaCl_2$	$MgCl_2$	EGTA	HEDTA	HEPES*
130 Cs^+	130	—	20	—	2	10	—	10
120 NMG^+	—	120	20	—	2	10	—	10
0·6 μM-Ca^{2+}	—	110	10	17·1	—	20	—	10
6 μM-Ca^{2+}	—	110	10	14·7	—	—	20	10

The osmolarity of all solutions was adjusted to 300 mosM with glucose. * pH was adjusted to 7·3 with CsOH. † *N*-methyl-D-glucamine.

Pulse protocols

After establishing the whole-cell clamp, cells were held at a potential varying between −70 and −90 mV. Current recording usually started 5 min later. Step depolarizations from the holding potential lasted 100–500 ms and were applied at intervals of 5–15 s to allow recovery from inactivation. Hyperpolarizing pulses (twenty to forty) were applied at 1/s after a series of step depolarizations, and the sequence was repeated every 5 min during the experiment. This allowed a more accurate compensation of leakage and capacitative currents, since they appeared to vary with time.

The condition of the cell during the experiment was controlled both by monitoring the d.c. level of membrane current at rest and by measuring the amplitude of Ca^{2+} currents at various potentials using short pulses repeated every 2–3 min. A steady leakage current of 20–30 pA, or a reduction of h.v.a. current to half of its initial size in 10 min were considered limiting conditions after which the cell was discarded.

External perfusion pipette

In experiments using ion substitution, test solutions were applied rapidly to the cell via a multi-barrelled pipette (Fig. 1*B*). The pipette was made of four heat-shrinkable needles, aligned and held together with a black thermo-contractive plastic tubing. The tubing was made long enough to cover the needles up to a distance of 6–7 mm from the tip. The uncovered part of the needles was then located and glued into a glass capsule of 5–6 mm in length as shown in Fig. 1*A*. The capsule was prepared under a microforge from soft glass of 1·6 mm in diameter and made with an opening of 50–100 μm at one end.

The perfusion pipette was normally placed about 50–100 μm from the cell. Three needles were used as inlet and one as outlet. If the outlet was open, the test solution was free to run in the pipette but not in the bath (Fig. 1*C*). If the outlet was stopped, the solution could rapidly flow out of the pipette by virtue of the small dead space at the tip and exchange the fluid surrounding the cell (Fig. 1*D*). The flow rate of the test solution was regulated hydrostatically. Flow rates of 20–50 μl/min were found to be optimum to achieve uniform perfusion and to preserve mechanical stability of the cell.

RESULTS

Activation–inactivation kinetics of Ca^{2+} currents

Fig. 2 shows a family of Ca^{2+} current recordings obtained during whole-cell clamp steps to various membrane potentials in chick (Fig. 2*A*) and rat d.r.g. cells (Fig. 2*B*) under normal ionic conditions. In both cases, l.v.a. currents turn on at about

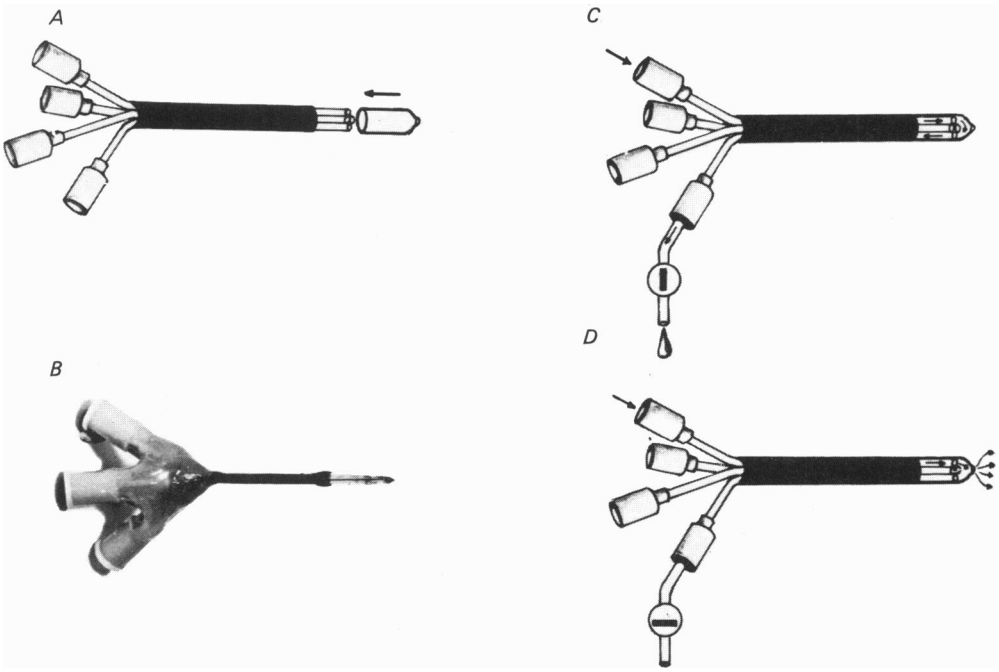

Fig. 1. A multi-barrelled ejection pipette employed for extracellular perfusion. *A*, schematic diagram showing the final stage of assembly of the pipette. *B*, photograph of the ejection pipette ready for use. *C* and *D*, diagram of the ejection system in shunted (*C*) and ejecting (*D*) modes.

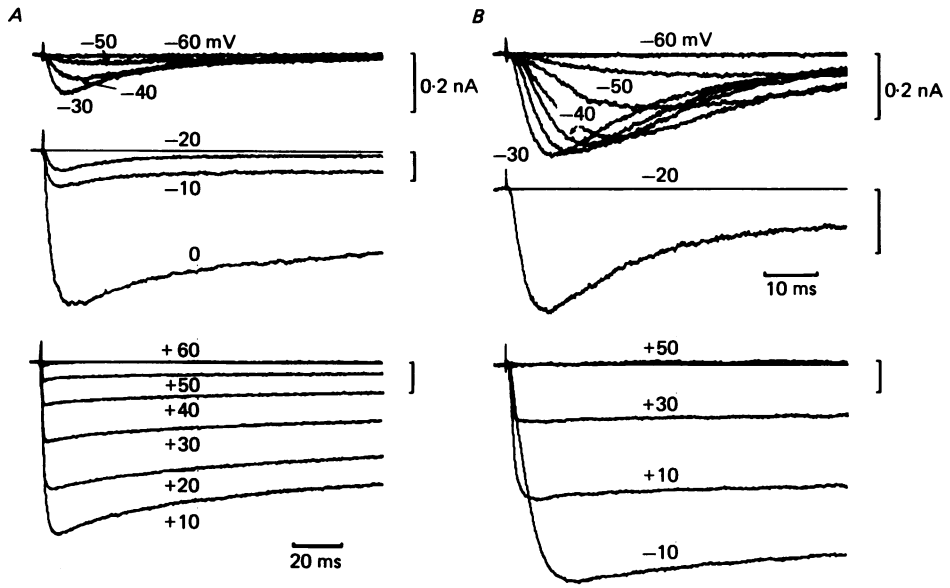

Fig. 2. Whole-cell clamp Ca^{2+} currents from chick (*A*) and rat (*B*) d.r.g. cells recorded at the membrane potential indicated. In *B* (top), step depolarizations from −60 to −30 mV were separated by 5 mV steps. For clarity intermediate curves at −55, −45 and −35 mV are not indicated. Vertical bars, 0·2 nA. Holding potential, −80 mV. Cell diameter: 10 μm (*A*), 15 μm (*B*). Out: 5 mM-Ca^{2+}. In: 130 mM-Cs^{+} (see Table 1).

−60 mV. Peak amplitude increases and activation accelerates with increasing membrane depolarization. In rat, there is a net increase in current noise at −50 mV which decreases at higher potentials (see top traces in Fig. 2*B*). Negative to −30 mV, activation of l.v.a. currents is sigmoidal and inactivation is fast and complete. Positive to −20 mV, where h.v.a. Ca^{2+} channels are activated, the kinetics of the Ca^{2+} current changes drastically. Between −20 and 0 mV, the peak amplitude increases considerably and current traces appear more noisy. At these potentials, activation becomes slower by a factor of two (Fig. 3*A*), but the rate of activation increases once again at more positive potentials. Inactivation is slower and incomplete and remains so at higher potentials.

To analyse the records of Fig. 2 quantitatively, we estimated three relevant parameters of the Ca^{2+} currents: (i) the peak Ca^{2+} current, I_p; (ii) the time to peak, t_p, as a measure of the activation kinetics; and (iii) the time constant of inactivation, τ_h, which was determined by fitting a single exponential to the falling phase of the current trace. Since activation of Ca^{2+} currents appeared to be much faster than inactivation at all membrane potentials, t_p and τ_h can be considered to represent a reasonably good estimate of activation and inactivation kinetics of Ca^{2+} currents. The results of this analysis from six cells are shown in Fig. 3*B–D*. The *I–V* characteristics (Fig. 3*B*) appear to have the typical double-peaked curve described previously (Carbone & Lux, 1984*a*). In chick d.r.g. cells (open circles), peak currents have steeper voltage dependency near −10 mV (5 mV for an e-fold change in I_p) than near −40 mV, where l.v.a. currents are activated (15 mV for an e-fold change in I_p). In rat d.r.g. cells (filled circles), the peak amplitude of l.v.a. currents at −30 mV is nearly twice as big as in chick, indicating a larger contribution of l.v.a. channels to the total Ca^{2+} current in these cells.

Between −50 and −30 mV, t_p and τ_h are sharply voltage dependent (Fig. 3*C* and *D*). In chick, at −50 mV an e-fold reduction of t_p (or τ_h) requires a 14 mV (or 9 mV) potential change. In rat, the two kinetic parameters are both smaller than in chick but less voltage dependent. Positive to −30 mV, both parameters assume unusual voltage dependencies. t_p increases abruptly between −20 and 0 mV followed by a continuous decrease at positive voltages. τ_h increases monotonically at more positive potentials, and such an increase correlates well with lowering of peak Ca^{2+} currents, suggesting a Ca^{2+}-dependent modulation of the h.v.a. channel inactivation (see Discussion).

At high voltages, τ_h was found to vary considerably from cell to cell. Cells having large currents (−1·2 to −1·8 nA) normally had a more pronounced inactivation (see e.g. the h.v.a. currents in an external Ca^{2+} concentration, $[Ca^{2+}]_o$, of 95 mM in Fig. 9). We rarely observed h.v.a currents of small amplitude (−0·2 to −0·4 nA) with strong inactivation. When this occurred, most of the residual inactivation of h.v.a. currents could be attributed to the presence of the l.v.a. component at these potentials.

τ_h of h.v.a. currents was found to be remarkably sensitive to the frequency of stimulation and to the holding potential. Frequent repetitions of the test pulse (1/s) produced a rapid lowering of current amplitudes and a marked slowing of Ca^{2+} current inactivation. Changing the holding potential from −90 to −60 mV also produced a decrease of peak Ca^{2+} currents and a slowing of the inactivation at +20 mV (Fig. 4*A* and *B*) as previously reported (Carbone & Lux, 1984*a*). The entire loss of

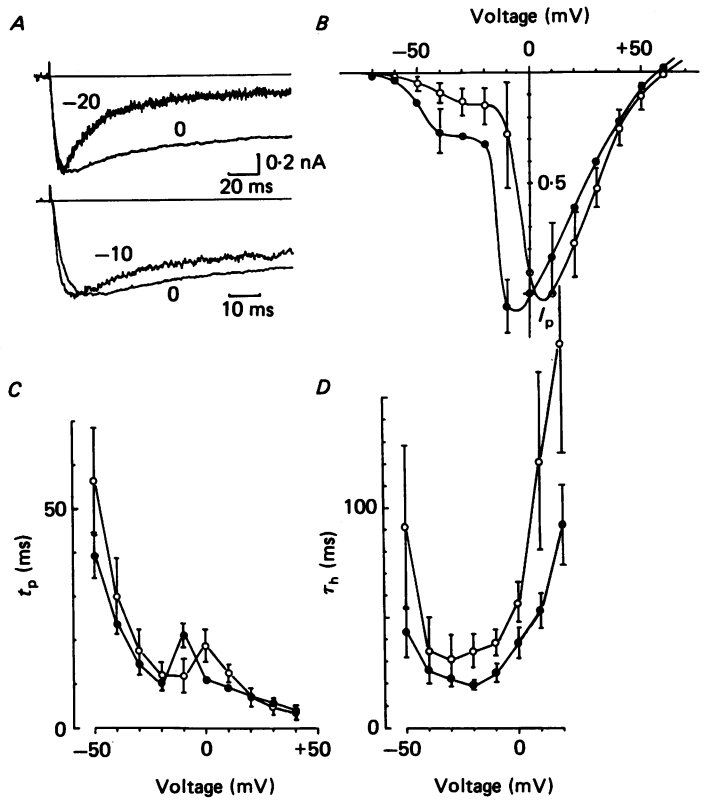

Fig. 3. *A*, comparison of the activation time course of the l.v.a. currents of Fig. 2*A*. Records at −20 and −10 mV are normalized to the peak amplitude of the current at 0 mV. *B*, *C* and *D*, normalized peak amplitude (I_p), time to peak (t_p) and inactivation time constant (τ_h) of Ca^{2+} currents from chick (○) and rat d.r.g. cells (●) *versus* voltage. τ_h was estimated by best fitting the decaying part of the Ca^{2+} current with a single exponential. The fitting started at the time when the Ca^{2+} current was 80% of its peak values (see also Fig. 10*A*). Points are averaged values over six cells. Bars denote standard deviations. Holding potential, −80 mV. Out: 5 mM-Ca^{2+}. In: 130 mM-Cs^+.

current at lower holding potentials was always larger than that attributable to the l.v.a component, which is shown to disappear already at holding potentials of −60 mV (Fig. 4*B*). This suggests that the h.v.a. current has a 'slow' voltage-dependent inactivation of its own, which may require more-positive potentials than used here to become complete. This explanation differs from that of Nowicky *et al.* 1985, who attribute the loss of current mostly to a third type of Ca^{2+} channel which is thought to be activated at potentials positive to +10 mV while being largely deactivated below −50 mV.

In our view, the apparently slower inactivation time course of h.v.a. currents at holding potentials of −60 mV (Fig. 4) is actually a consequence of the increased steady-state inactivation of l.v.a. channels which also contributes to the fast-inactivating time course of Ca^{2+} currents at high voltages. This is shown in Fig. 4*D*, where the difference between the h.v.a. current at +20 mV from holding potentials

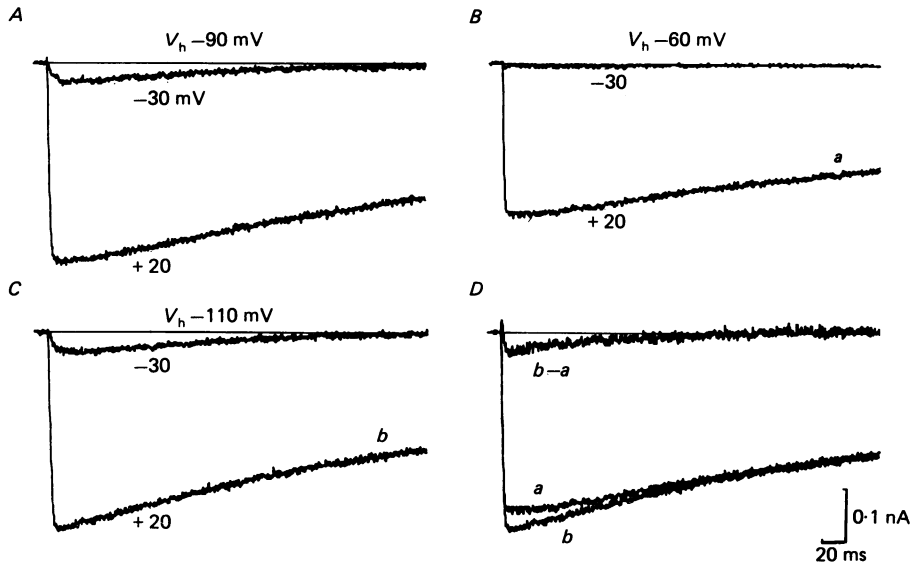

Fig. 4. *A*, *B* and *C*, time course of l.v.a. and h.v.a. currents elicited from −90, −60 and −110 mV holding potentials (V_h). The cell was maintained for 3 min at each holding potential before depolarizing pulses to −30 and +20 mV were delivered. The holding potentials were applied in the same order as shown: −90, −60 and −110 mV. *D*, records *a* and *b* are those indicated in parts *B* and *C* of this Figure and their algebraic difference is shown as *b* − *a*. Record *a* is multiplied by a factor of 1·2 to correct for the 20 % steady-state inactivation of h.v.a. channels at −60 mV. The cell was a chick d.r.g. cell of 13 μm diameter. 2·5 kHz low-pass filter. Out: 5 mM-Ca^{2+}. In: 130 mM-Cs^+.

of −110 mV (*b*) and −60 mV (*a*), is recorded after appropriate correction for the loss of h.v.a. currents (trace *b* − *a*). As shown, the difference in current shows fast inactivation and its size is comparable to the l.v.a. current activated at −30 mV.

Recovery from inactivation

L.v.a., but not h.v.a., currents can be completely inactivated when the cell is maintained for a sufficiently long period of time at a holding potential of −50 mV (Fig. 5; see also Carbone & Lux, 1984*a*). Step depolarizations from such a holding potential solely elicit the h.v.a. currents (Fig. 5*B*), but not the l.v.a. currents (Fig. 5*A*). L.v.a. channels recovered from inactivation, provided that the cell was hyperpolarized to more-negative membrane potentials for a sufficiently long period of time (see Fig. 5*C*). Step depolarizations to −50 mV following a pre-hyperpolarization of 500 ms to −100 mV activate an l.v.a. current with an amplitude of about 0·1 nA.

As with Na^+ channels, recovery from inactivation of l.v.a. channels is time- and voltage-dependent. This is illustrated by the Ca^{2+} currents recorded on step depolarizations to −30 mV following conditioning pulses of variable duration (ΔT) to −80, −100 and −120 mV (Fig. 6). At −80 mV, the amplitude of the Ca^{2+} current increases exponentially with a time constant of 1·5 s (τ_r). At −120 mV, recovery from inactivation is faster and τ_r is about half of that at −80 mV. In three other cells, τ_r averaged 1·2 ± 0·3 s (mean ± S.D.) at −80 mV and 0·7 ± 0·2 s at −120 mV.

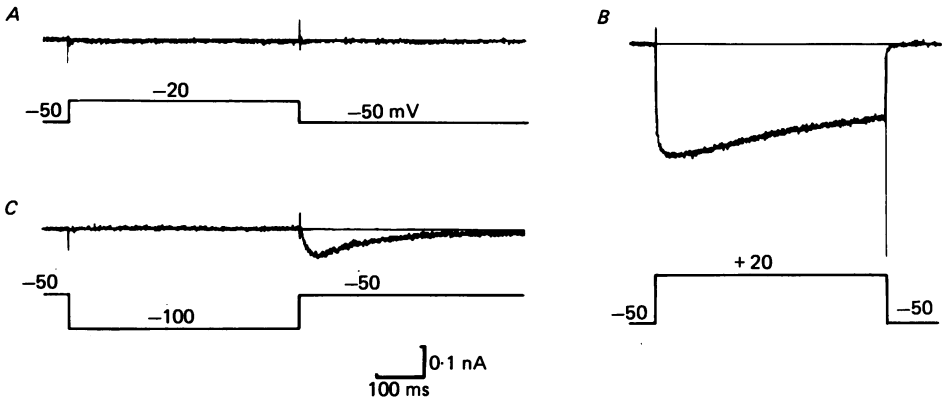

Fig. 5. Recovery from inactivation of l.v.a. channels in a chick d.r.g. cell. *A* and *B*, Ca^{2+} currents elicited on step depolarizations to −20 and +20 mV from a holding potential of −50 mV. The pulse protocol is indicated below each current trace. The inward current at +20 mV is of the h.v.a. type. *C*, l.v.a. current obtained on repolarization to −50 mV after a 500 ms pre-hyperpolarization to −100 mV. Out: 5 mM-Ca^{2+}. In: 130 mM-Cs^{+}.

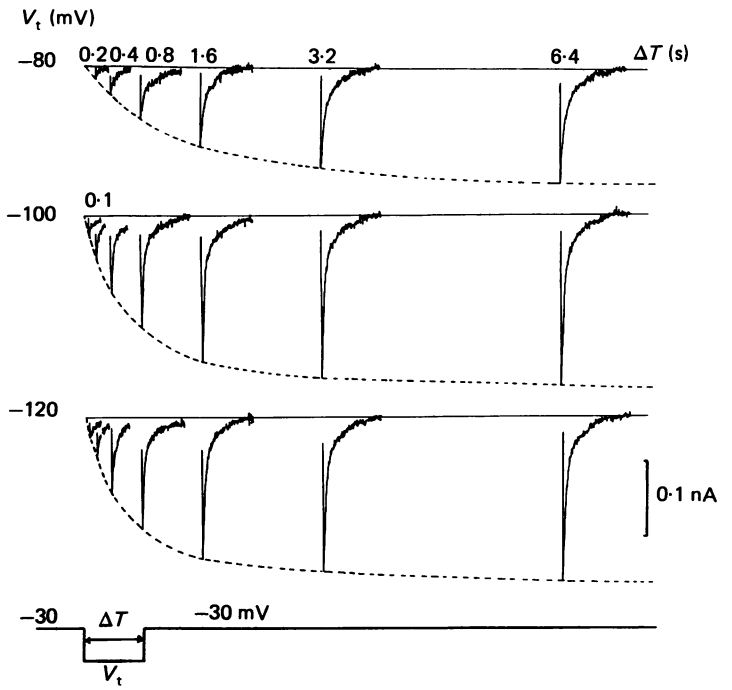

Fig. 6. Time course of recovery from inactivation of l.v.a. channels at various membrane repolarizations. Records represent l.v.a. currents measured on depolarization to −30 mV after pre-hyperpolarizations to the test potential, V_t, of variable length (ΔT). V_t is indicated on the left, and ΔT on the top part of the Figure. The cell was held at rest at −30 mV. The dashed curves are single exponentials with time constants 1·4 s (−80 mV), 0·6 s (−100 mV) and 0·4 s (−120 mV). The cell was a chick d.r.g. cell with 15 μm diameter. Out: 5 mM-Ca^{2+}. In: 130 mM-Cs^{+}.

Tail currents

Tail currents associated with the closing of l.v.a. channels could be fitted by a single exponential with time constant τ_t that decreased at negative potentials (Fig. 7*A*). τ_t, measured at the peak of Ca^{2+} activation, was 5·6 ms at −70 mV (trace *b*, inset), and was nearly four times shorter (1·2 ms, trace *d*) at −100 mV. Tail currents associated with h.v.a. channels also decayed exponentially and accelerated at more-negative membrane potentials (Fig. 7*B*) (see also Fenwick, Marty & Neher,

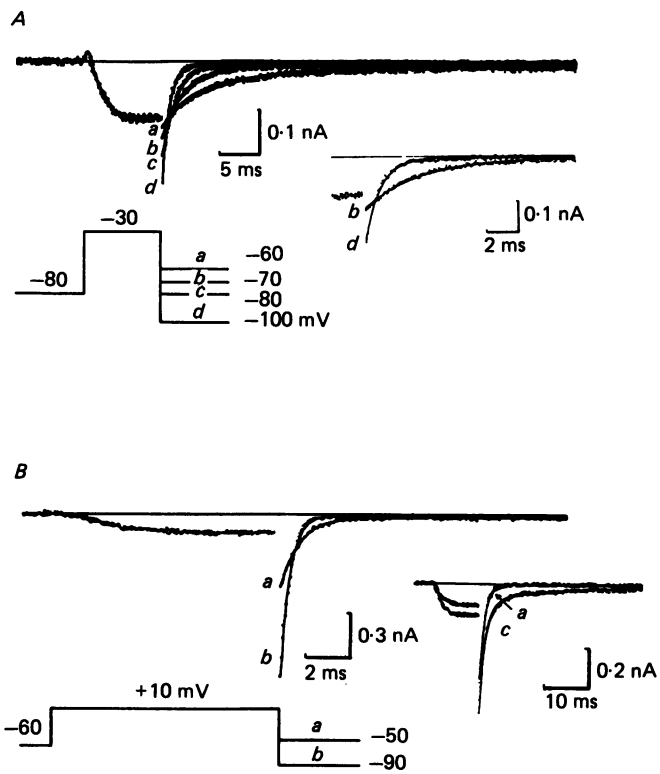

Fig. 7. Turn-off of Ca^{2+} currents in a chick d.r.g. cell. *A*, l.v.a. tail currents associated with step repolarizations to −60 mV (curve *a*), −70 mV (*b*), −80 mV (*c*) and −100 mV (*d*). The pulse protocols are indicated below the current traces. The time constants of the tail currents (τ_t) were calculated by fitting an exponential function to the tail recordings and omitting the initial 150 μs and the last 10% of the decline. The τ_t values are 7·8 ms (curve *a*), 5·6 ms (*b*), 3·4 ms (*c*) and 1·2 ms (*d*). Inset to *A*, tail currents associated with repolarizations to −70 and −100 mV on an expanded time scale. Best-fitting curves are superimposed on the original traces. Holding potential, −80 mV. Test potential, −30 mV. *B*, h.v.a. tail currents associated with step repolarizations to −50 mV (*a*) and −90 mV (*b*). Data are from a different cell. The cell was maintained at a holding potential of −60 mV for 5–10 min to cause full inactivation of l.v.a. channels. Test depolarizations to +10 mV. The τ_t values are 0·58 ms (*a*) and 0·4 ms (*b*). Inset to *B*, tail currents on repolarizations to −50 mV from holding potentials of −60 mV (*a*) and −90 mV (*c*). Test depolarizations to +10 mV. Trace *a* coincides with that in the main Figure. Trace *c* is fitted by a double exponential $A_1 \exp(-t/\tau_1) + A_2 \exp(-t/\tau_2)$ with $A_1 = -0{\cdot}39$ nA, $A_2 = -0{\cdot}07$ nA, $\tau_1 = 1{\cdot}01$ ms and $\tau_2 = 9{\cdot}7$ ms. 5 kHz low-pass filter. Sampling rate 50 μs. Out: 5 mM-Ca^{2+}. In: 130 mM-Cs^+.

1982). At −50 mV, τ_t was 0·58 ms (trace *a*), which decreased to 0·4 ms at −90 mV (trace *b*). These observations suggested that closing of h.v.a. channels is less voltage dependent and occurs at rates five to ten times faster than that of l.v.a. channels. In this experiment the cell was held at −60 mV to minimize the contribution of l.v.a. channels. As shown in the inset of Fig. 7*B*, activation of l.v.a. channels alters the time course of tail currents. Trace *c* is obtained under the same conditions as trace *a* except that the cell was first hyperpolarized to −90 mV for 3 min before applying the test pulse. Trace *c* appears to have a slow component (see legend), most likely associated with the closing of l.v.a. channels, which may have recovered from inactivation during the 3 min of pre-conditioning at −90 mV.

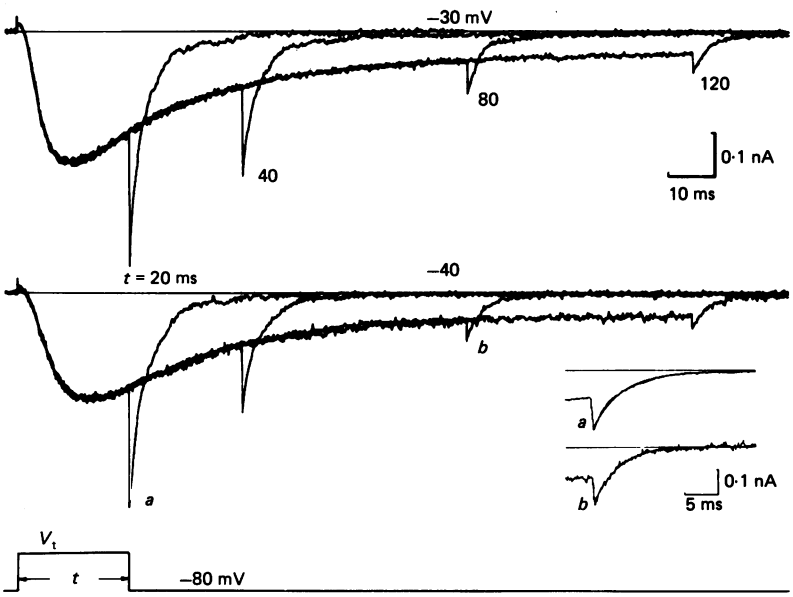

Fig. 8. Development of l.v.a. tail currents with pulse duration in a rat d.r.g. cell. Ca^{2+} tail currents were obtained on repolarization to −80 mV following depolarizations to −30 mV (top) and −40 mV (bottom) of variable duration (*t*). The value of *t* is given near each tail current. The pulse protocol is indicated at the bottom. Holding potential, −80 mV. The time constant of tail currents, τ_t, was calculated with a procedure similar to Fig. 7. The τ_t values are: 3·2 ms (at 20 ms), 3·1 ms (40 ms), 2·8 ms (80 ms) and 2·7 ms (120 ms) at −30 mV, and 3·4 ms (20 ms), 3·3 ms (40 ms), 3·0 ms (80 ms) and 2·4 ms (120 ms) at −40 mV. Inset, initial parts of the tail currents, *a* and *b*, plotted on an expanded scale. Trace *b* is normalized to trace *a*. Best-fitting curves are superimposed on the original records. Recording conditions as in Fig. 7. Out: 20 mM-Ca^{2+}. In: 130 mM-Cs^+.

Tail currents associated with step repolarizations to −80 mV, following depolarizations of variable duration, have different amplitudes but similar time constants (Fig. 8). This is more evident in the inset to Fig. 8 where the tail currents recorded are plotted after step depolarizations to −40 mV, lasting 20 (*a*) and 80 ms (*b*). The two traces are scaled and fitted with single exponential functions of time constants 3·2 (*a*) and 2·8 ms (*b*). This suggests that irrespective of their amplitude, the time course of tail currents appears to be independent of the level and duration of the preceding depolarization. This agrees with recent observations on a similar Ca^{2+} channel ('slow deactivating') in clonal pituitary cells (Matteson & Armstrong, 1986).

Effects of extracellular Ca^{2+} on l.v.a. currents

At low membrane potentials (−50 and −20 mV), elevations of $[Ca^{2+}]_o$ from 5 to 95 mM cause a 60–70 % increase in the amplitude of Ca^{2+} currents with little change in the activation–inactivation kinetics (Fig. 9). At more-positive potentials, Ca^{2+} currents undergo a similar increase, but the inactivation kinetics appear to be faster by a factor of 2 to 3. This finding is consistent with the view that inactivation of h.v.a.

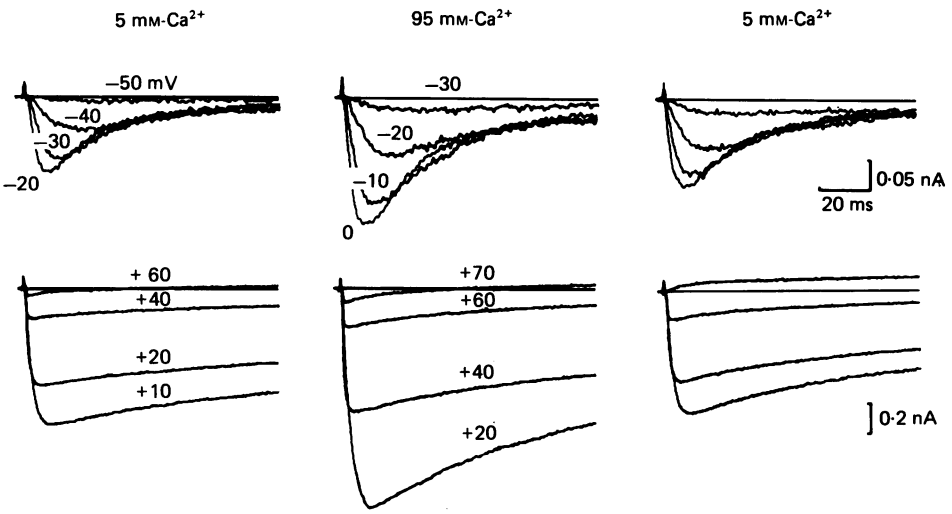

Fig. 9. Time course of l.v.a. (top) and h.v.a. (bottom) currents in 5 and 95 mM-Ca^{2+} from a chick d.r.g. cell. Step depolarizations from the holding potential are indicated near each trace. Holding potential, −80 mV. Cell diameter, 15 μm. 2·5 kHz low-pass filter. In: 130 mM-Cs^+.

channels is somehow affected by the rate of Ca^{2+} entry into the cell (see Eckert & Chad, 1984). In Fig. 10 *B–D* the voltage dependence of I_p, t_p and τ_h is shown for the current traces of Fig. 9. Apart from a voltage shift of about 17 mV to the right, owing to a positive increase of the membrane phase boundary potential (secondary to elevations of the divalent cation concentration), the voltage dependence of all three parameters is little changed in the presence of a $[Ca^{2+}]_o$ of 95 mM (Fig. 10).

Careful examination of Figs. 9 and 10 reveals that activation and inactivation kinetics of l.v.a. channels are independent of the magnitude of Ca^{2+} currents, ruling out the possibility that Ca^{2+} entry can directly affect the gating mechanism of l.v.a. channels. This is seen better in Fig. 10 *A*, where two current traces in 5 and 95 mM-Ca^{2+}, activated at −20 and 0 mV respectively, are superimposed. The two traces are taken at different membrane potentials in order to account for the 20 mV voltage shift seen when altering $[Ca^{2+}]_o$. Despite the increase in peak amplitude, the current at 0 mV has nearly the same time to peak and time constant of inactivation as that at −20 mV (see Fig. 10 legend). The peak currents decreased by a factor of about 3 when $[Ca^{2+}]_o$ was lowered from 5 to 1 mM (Fig. 11). The time courses of activation and inactivation remained fairly constant when accounting for a negative voltage shift of 10 mV for activation at a $[Ca^{2+}]_o$ of 1 mM. The normalized amplitudes of l.v.a. and

h.v.a. currents measured at various Ca^{2+} concentrations are plotted in Fig. 11*C*. Both currents appear to have similar relationships with $[Ca^{2+}]_o$. They can both be fitted by a function representing the fraction of binding sites occupied by a calcium ion assuming a one-to-one ion receptor site reaction. A similar relationship was also found for the h.v.a. current of *Helix* neurones (Akaike, Lee & Brown, 1978).

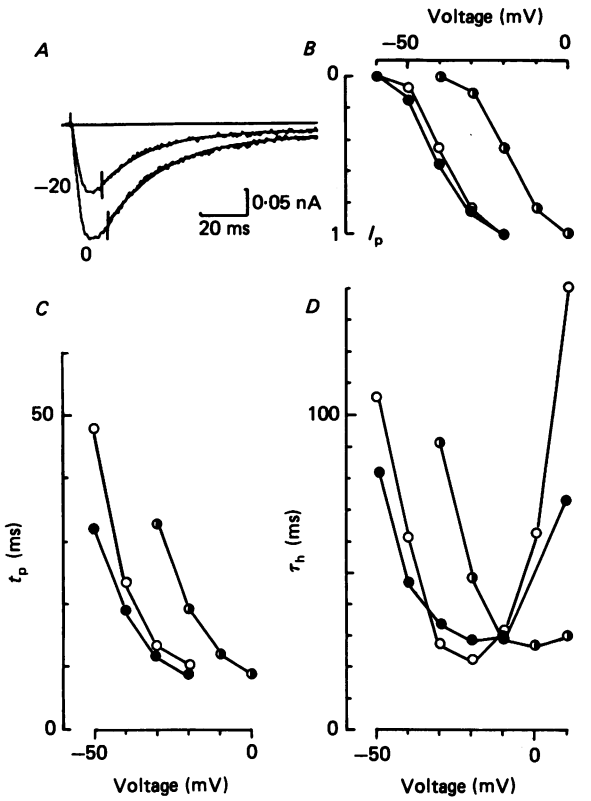

Fig. 10. Kinetic parameters in 5 and 95 mM-external Ca^{2+}. *A*, superimposed l.v.a. current records taken from Fig. 9 at 5 mM-Ca^{2+} (−20 mV) and 95 mM-Ca^{2+} (0 mV). Traces are fitted with a single exponential with time constant 27 ms (0 mV) and 22 ms (−20 mV). The beginning of the fitting is indicated by a vertical bar on each trace. Despite a larger peak amplitude, the trace at 0 mV has a slower relaxation. *B*, *C* and *D*, plot of I_p, t_p and τ_h *versus* voltage, in 5 mM-Ca^{2+} (control, ○), 95 mM-Ca^{2+} (◑) and 5 mM-Ca^{2+} (recovery, ●). Peak amplitudes are plotted normalized to the maximum amplitude of l.v.a. currents.

Separation of l.v.a. from h.v.a. currents

Fig. 12*A* shows a series of current recordings obtained during intracellular dialysis of a chick d.r.g. cell with 130 mM-CsF. The current traces are substantially different from those of cells maintained in normal ionic conditions (see Figs. 2 and 9). At potentials more positive than −20 mV, there is no sign of the abrupt increase in Ca^{2+} currents due to the activation of h.v.a. channels. At potentials more negative than

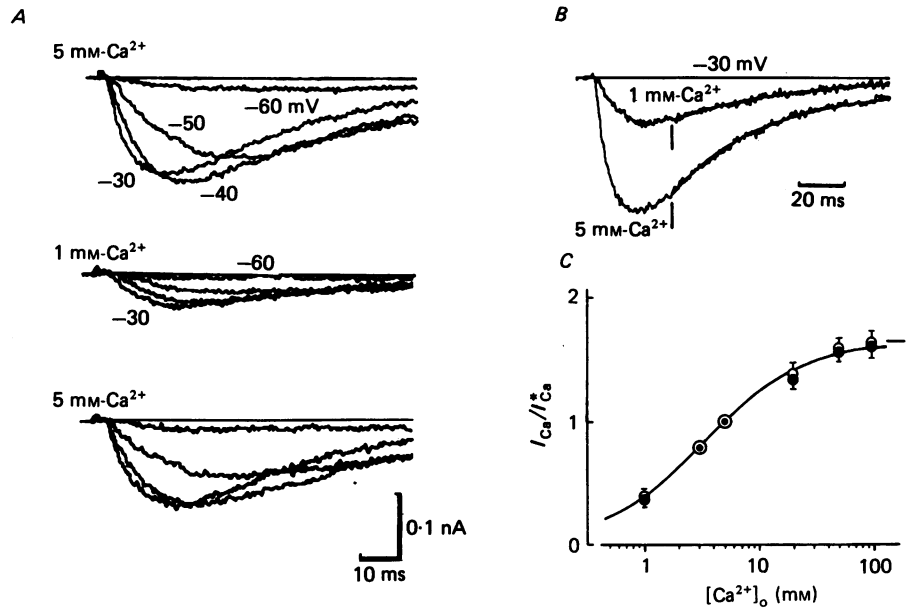

Fig. 11. *A*, time course of l.v.a. currents in 1 and 5 mM-external Ca^{2+} in a chick d.r.g. cell. Test potentials are indicated near each trace. Out: 5 or 1 mM-Ca^{2+}. In: 130 mM-Cs^{+}. *B*, comparison of the time course of l.v.a. currents from *A* at −30 mV in 1 and 5 mM-external Ca^{2+}. The falling phase of the currents is fitted by a single exponential with time constant 38·2 ms (5 mM-Ca^{2+}) and 48·8 ms (1 mM-Ca^{2+}). Bars indicate the beginning of the fitting. *C*, maximum peak Ca^{2+} currents *versus* $[Ca^{2+}]_o$. Filled circles refer to means (n = 4–8) of l.v.a. currents of different cells; open circles refer to means of h.v.a. currents of the same cells. All data are normalized to a $[Ca^{2+}]_o$ of 5 mM which is the control concentration in all experiments. The continuous line is the result of a curve fit using the equation:

$$I_{Ca}/I^{*}_{Ca} = \frac{I_{Ca,max}/I^{*}_{Ca}}{1+K_D/[Ca^{2+}]_o},$$

where I_{Ca} and I^{*}_{Ca} are the peak currents at a given Ca^{2+} concentration and at 5 mM-Ca^{2+}, respectively. K_D is the dissociation constant of the calcium binding site. $I_{Ca,max}$ is the peak current when all the sites are occupied by Ca^{2+}. In our case, K_D is 3·3 mM and $I_{Ca,max}/I^{*}_{Ca}$ is 1·7. Note that the continuous line fits both open and filled symbols well.

−30 mV, peak current increases with increasing membrane depolarizations to decrease again at higher potentials (see inset in Fig. 12*B*). Inactivation time constant and time to peak decrease monotonically with voltage (Fig. 12*B* and *C*). These findings indicate that internal perfusion with F^{-} is effective at suppressing h.v.a. channels irreversibly. Indeed, l.v.a. currents were also reduced in the presence of intracellular F^{-}, although to a smaller degree. The reversal potential measured for Ca^{2+} currents drifted continuously towards more-negative potentials and leakage currents increased signficantly. These drawbacks made this method inconvenient for a routine separation of l.v.a. from h.v.a. currents.

Separation of l.v.a. from h.v.a. channels was better achieved when d.r.g. cells were perfused with intracellular solutions containing high Ca^{2+} (10^{-7}–10^{-5} M) (Carbone & Lux, 1985; Bossu *et al.* 1985). Fig. 13 shows two examples of Ca^{2+} currents recorded

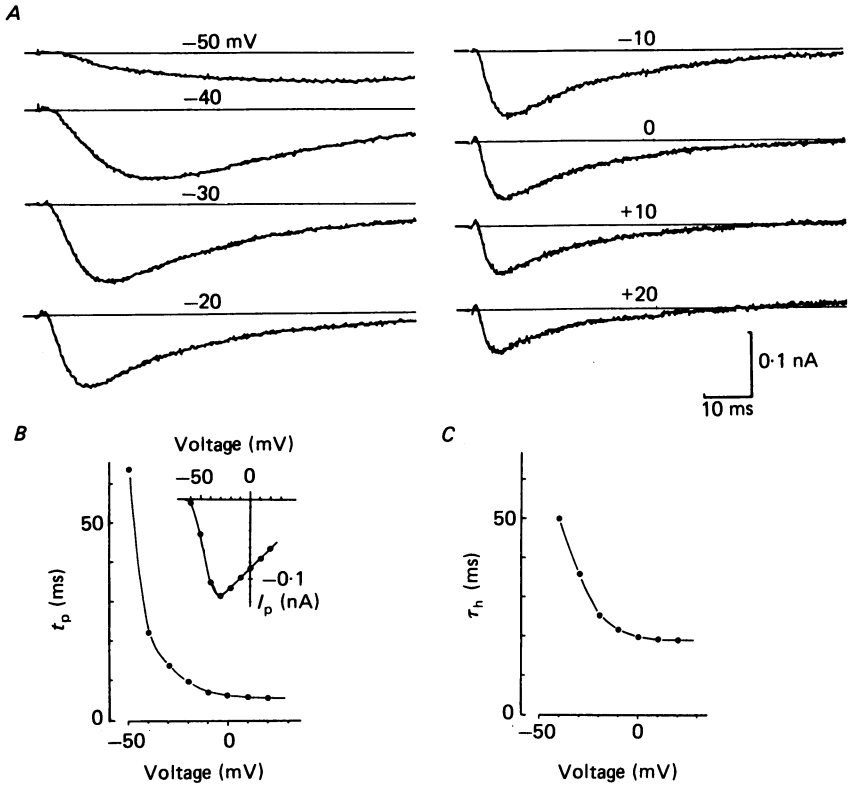

Fig. 12. *A*, l.v.a. currents from a chick d.r.g. cell perfused with 130 mM-CsF at the potential indicated. Records were taken from approximately 15 min after establishment of the whole-cell clamp. *B* and *C*, t_p and τ_h calculated from the above records *versus* voltage. Inset in B: I_p *versus* voltage. Cell diameter, 10 μm. 2·5 kHz low-pass filter. Out: 5 mM-Ca^{2+}.

from cells perfused with an intracellular Ca^{2+} concentration, $[Ca^{2+}]_i$, of 0·6 μM (*A*) and 6 μM (*B*). In Fig. 13*A*, h.v.a. currents are strongly reduced but not completely abolished by a $[Ca^{2+}]_i$ of 0·6 μM. t_p increases by a factor of 2 on changing the membrane potential from −30 to −20 mV, and current inactivation remains fairly incomplete above −20 mV. Complete suppression of h.v.a. channels occurred at higher $[Ca^{2+}]_i$ (6 μM), as shown in Fig. 13*B*. Under these conditions, there was no sign of slowly inactivating Ca^{2+} currents at any potential tested. Rather, Ca^{2+} currents were fully inactivating even at +50 mV. Similar results were also found when $[Ca^{2+}]_i$ was increased by one to two orders of magnitude using Ca^{2+}–NTA buffers, or unbuffered solutions.

Another way to separate l.v.a. from h.v.a. channels was to take advantage of the fact that under standard ionic conditions h.v.a. channels are known to 'run-down' faster than l.v.a. channels (see Methods). Thus in cells having low levels of leakage currents, pure l.v.a. currents could be recorded just by waiting 20–40 min after the start of internal perfusion. Such an example is illustrated in Fig. 14. A series of Ca^{2+} currents recorded soon after the establishment of the whole-cell configuration in a rat d.r.g. cell is shown in Fig. 14*A*. 25 min later, Ca^{2+} currents also appeared to inactivate fully at very positive potentials (Fig. 14*B*), consistent with the idea that

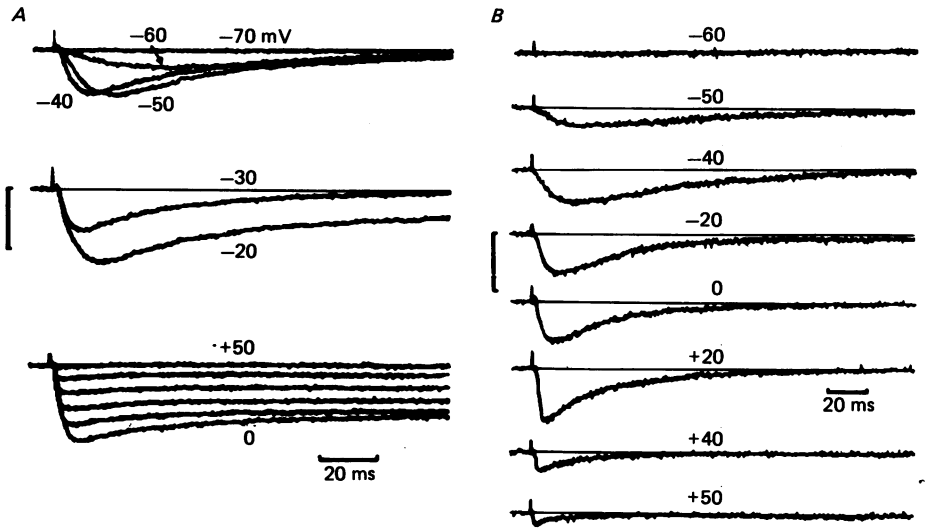

Fig. 13. Effects of increasing the intracellular free Ca^{2+} concentration ($[Ca^{2+}]_i$) on the time course of Ca^{2+} currents in chick d.r.g. *A*, Ca^{2+} currents in the presence of a $[Ca^{2+}]_i$ of 0·6 μM. Current traces were obtained from approximately 5 min after the establishment of whole-cell recording. Internal Cs^+ was replaced with NMG (*N*-methyl-D-glucamine) to minimize outward current components (see Table 1). Bottom records obtained between 0 and +50 mV were separated by steps of 10 mV. Vertical bars, 0·2 nA. Cell diameter, 12 μm. Out: 5 mM-Ca^{2+}. In: 120 mM-NMG^+. *B*, Ca^{2+} currents in $[Ca^{2+}]_i$ of 0·6 μM from a different cell. Similar conditions as in *A*. Cell diameter, 14 μm.

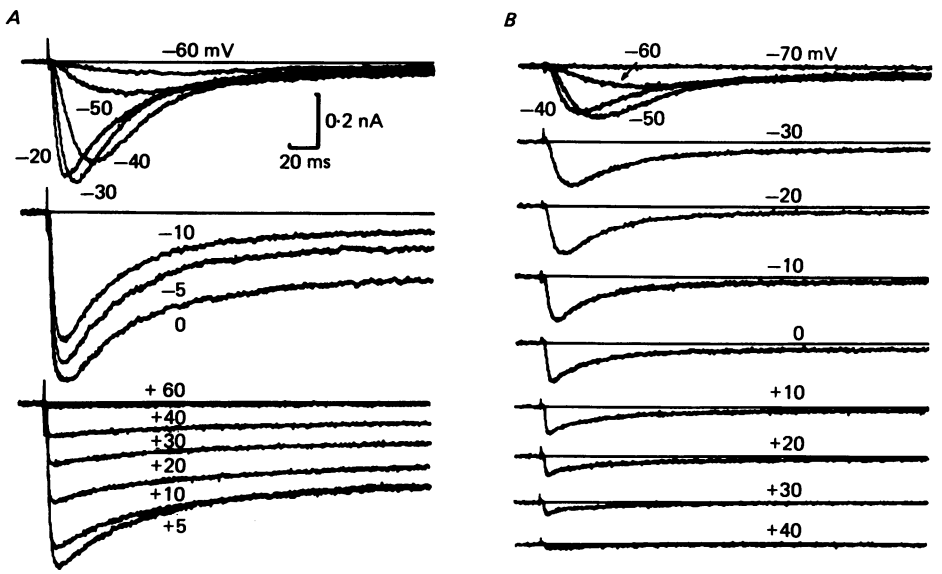

Fig. 14. Run-down of h.v.a. currents in a rat d.r.g. cell under standard ionic conditions. *A*, current traces obtained at the membrane potential indicated soon after establishment of the whole-cell clamp conditions. Notice the relatively small amplitude of the h.v.a. component compared to normal rat d.r.g. cells (Fig. 2). *B*, current traces after about 30 min from recordings in *A*. Holding potential, −80 mV. Cell diameter, 15 μm. Out: 20 mM-Ca^{2+}. In: 120 mM-NMG^+.

only l.v.a. channels were operative under these conditions. Peak amplitude increases gradually up to −40 mV, decreasing again at higher voltages. t_p and τ_h become monotonically voltage dependent (Fig. 15) and I_p loses the double-peaked shape to assume the classical single-peaked *I–V* characteristic expected for a voltage-dependent channel which activates at around −50 mV and has a reversal equilibrium potential at about +50 mV (inset in Fig. 15). To be sure that the run-down of the h.v.a. channel was complete, Verapamil was added to the bath in doses of 50 and 100 μM, doses which are known to block the h.v.a. current fully without affecting the l.v.a. currents significantly (Boll & Lux, 1985).

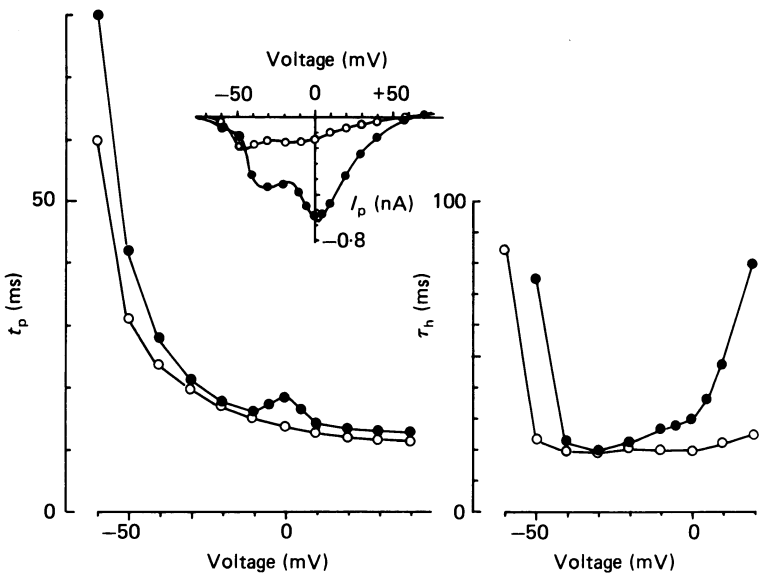

Fig. 15. t_p (*V*) and τ_h (*V*) before and after the run-down of h.v.a. current shown in Fig. 14. Filled circles refer to Fig. 14*A*; open circles refer to Fig. 14*B*. Inset, I_p *versus* voltage. The *I–V* characteristic after 30 min perfusion (open circles) is shifted nearly 10 mV to the left.

Selectivity to divalent cations

L.v.a. and h.v.a. currents could be reversibly blocked by replacing Ca^{2+} with Ni^{2+} in the external solution (Fig. 16). In 5 mM-Ni^{2+}, block of l.v.a. and h.v.a. channels was complete and required only a few seconds to reach steady-state equilibrium conditions. Recovery was also rapid and complete after wash-out of the Ni^{2+}-containing solution (Fig. 16, right). Application of 100 μM-Cd^{2+} had similar effects.

The effects on Ca^{2+} currents of replacing external Ca^{2+} with Ba^{2+} are shown in Fig. 17. In 20 mM-Ba^{2+}, the time course of l.v.a. currents is practically unchanged, while the peak current is reduced by about 30%, suggesting a reduced permeability of Ba^{2+} through open l.v.a. channels. Ba^{2+} currents through h.v.a. channels, on the other hand, are nearly doubled in 20 mM-Ba^{2+}. The reversal potential for Ba^{2+} currents (+70 mV) is almost the same as for Ca^{2+}. The time course of inactivation also appears only slightly slower. This is similar to previous published observations on the

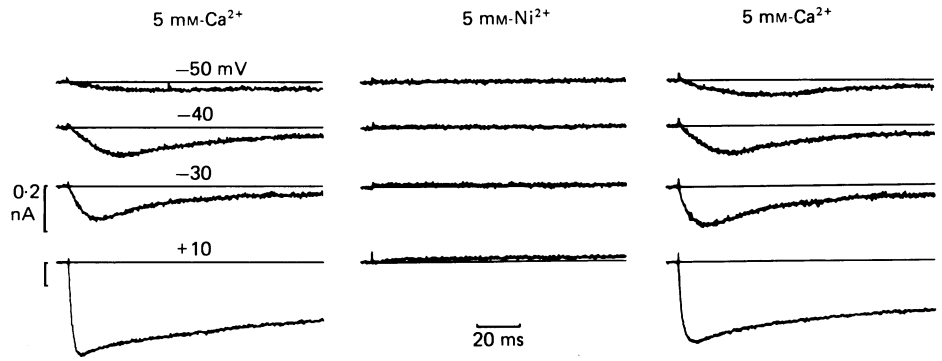

Fig. 16. Block of Ca^{2+} currents by Ni^{2+} in a chick d.r.g. cell. L.v.a. and h.v.a. currents before (left), during (middle) and after (right) application of 5 mM-Ni^{2+} to the external bath. Step depolarizations are indicated on the left. The effects of Ni^{2+} and recovery were complete within seconds. Holding potential, −80 mV. Cell diameter, 10 μm. Out: 5 mM-Ca^{2+} or Ni^{2+}. In: 130 mM-Cs^{+}.

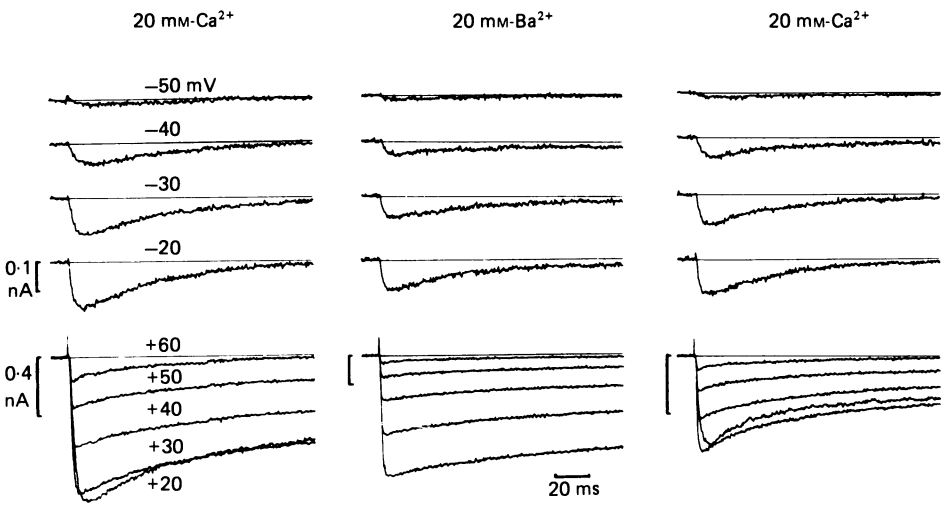

Fig. 17. Time course of l.v.a. (top) and h.v.a. (bottom) currents in 20 mM-Ba^{2+} from a chick d.r.g. cell. At control, the cell was bathed in a solution containing 20 mM-Ca^{2+} (left). The bath was then changed to 20 mM-Ba^{2+} (middle). Records were taken after nearly 1 min of perfusion in 20 mM-Ba^{2+}. On the right are Ca^{2+} currents after 3 min washing in 20 mM-Ca^{2+}. Notice the different vertical scales for the h.v.a. currents (bottom traces). H.v.a. currents nearly double in 20 mM-Ba^{2+} and have slower inactivation. Holding potential, −80 mV. Cell diameter, 12 μM. 2·5 kHz low-pass filter. In: 130 mM-Cs^{+}.

classical Ca^{2+} channel (Hagiwara & Byerly, 1981; Fedulova *et al.* 1985) and reinforces the view that l.v.a. and h.v.a. channels have different selectivity for divalent cations.

Replacement of Ca^{2+} with Sr^{2+} did not produce significant changes in the time course of l.v.a. and h.v.a. currents (Fig. 18), but Sr^{2+} increased the peak amplitude of both currents by nearly 20 %, suggesting a larger permeability to Sr^{2+} through these channels.

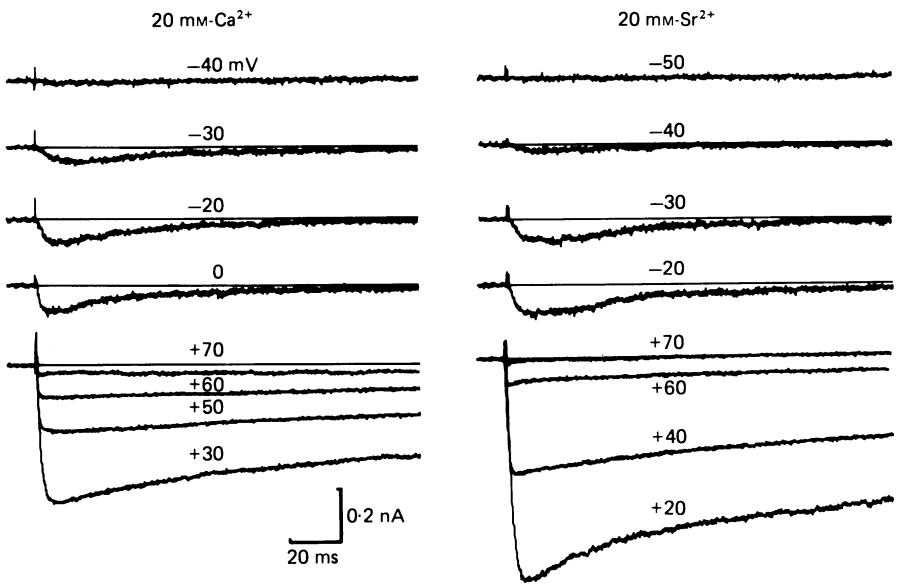

Fig. 18. Ca^{2+} currents in 20 mM-Sr^{2+} recorded at the membrane potentials indicated. The experiment was performed as described in Fig. 17. Current traces after washing in 20 mM-Ca^{2+} were very similar to those at control (not shown). Holding potential, −80 mV. 2·5 kHz low-pass filter. In: 130 mM-Cs^{+}.

DISCUSSION

Previous reports on the properties of Ca^{2+} channels in vertebrate sensory neurones consistently showed the existence of a second population of Ca^{2+} channels that is activated at more-negative potentials than those reported for the classical Ca^{2+} channel (Carbone & Lux, 1984*a*; Fedulova *et al.* 1985; Bossu *et al.* 1985; Nowycky *et al.* 1985). Observations on l.v.a. channels, however, have been limited to a narrow range of membrane potentials (−50 to −20 mV) because the activation of the classical Ca^{2+} channel makes an independent analysis difficult. Our results on isolated l.v.a. currents extend these previous observations to a wider range of membrane potentials (−50 to +40 mV) and furnish a more complete picture of the activation–inactivation mechanism of this channel. Our findings led us to conclude that the activation and inactivation time course of l.v.a. currents is controlled by voltage-dependent gates. Ca^{2+}, Ba^{2+} and Sr^{2+} but not Mg^{2+} permeate at comparable rates through open l.v.a. channels, while metallic bivalent ions such as Ni^{2+} and Cd^{2+} block the channel. L.v.a. currents are larger in rat than in avian d.r.g. cells.

On–off gating of l.v.a. channels

In agreement with previous reports (Carbone & Lux, 1984*a*; Fedulova *et al.* 1985; Bossu *et al.* 1985), activation of l.v.a. channels in sensory neurones is sigmoidal and voltage dependent. At −50 mV, t_p is 50–60 ms and decreases e-fold with a 14 mV increase in membrane potential (Fig. 3*C*). Between −20 and 0 mV, t_p (V) shows a sharp discontinuity (Fig. 3*C*), which disappears when h.v.a. channels are suppressed

by internal applications of high $[Ca^{2+}]_i$ and F^- (Figs. 12 and 13). Discontinuity in t_p (V) has also been shown for the l.v.a. currents of adult rat d.r.g. cells (Fedulova *et al.* 1985), and as such it can be taken as an indication for the coexistence of two types of Ca^{2+} channels in the plasma membrane.

In separated l.v.a. currents, t_p decreases monotonically with increasing voltages (−50 to +40 mV), suggesting that activation of l.v.a. channels obeys kinetic schemes similar to those of other classical voltage-dependent channels. Consistent with this view is also the observation that the turn-off of l.v.a. channels can be fitted by a single exponential, whose time constant is independent of the level and duration of the test pulse (Figs. 7 and 8). The time constants of l.v.a. tail currents (3–3·4 ms at −80 mV, 20–22 °C) compare well with previous data at lower temperature (5 ms at −80 mV, 12 °C; Carbone & Lux, 1984*a*), and with those of the slowly deactivating Ca^{2+} channel in clonal pituitary cells (3 ms at −80 mV, 18–20 °C; Matteson & Armstrong, 1986). As in pituitary cells, closing of l.v.a. channels is approximately one order of magnitude slower than that of h.v.a. channels. This is the reason for the double-exponential time course of tails recorded at low voltages (−90 mV), where both channels are simultaneously active.

Inactivation of l.v.a. channels is not Ca^{2+} dependent

Several lines of evidence indicate that inactivation of l.v.a. channels is voltage- and not Ca^{2+}-dependent. (i) In chick d.r.g. cells under normal ionic conditions, the time constant of inactivation, τ_h, decreases nearly 3-fold by changing the potential from −50 to −30 mV (Fig. 3*D*). This is also evident in isolated l.v.a. currents where τ_h assumes a clear monotonic voltage dependence between −50 and +20 mV (Figs. 12 and 15). (ii) An increase in Ca^{2+} current following elevations of $[Ca^{2+}]_o$ from 5 to 95 mM, produces only a voltage shift of τ_h (V). There are no accelerations of the inactivation time course as expected by the rapid rise of $[Ca^{2+}]_i$ at all potentials. (iii) Inactivation of l.v.a. channels remains fast and insensitive to elevations of $[Ca^{2+}]_i$ to levels of 1×10^{-6} to 1×10^{-5} M (Fig. 13). Thus, we conclude that inactivation of l.v.a. channels is merely voltage gated and is neither influenced by the rate of Ca^{2+} entry nor by the level of free intracellular Ca^{2+}.

In contrast to the l.v.a. channel, inactivation of the h.v.a. channel appears to be dependent on the rate of Ca^{2+} entry. This is similar to other preparations (see Eckert & Chad, 1984, for a review) and is supported by the following observations. (i) At potentials more positive than −10 mV, where h.v.a channels are normally activated, τ_h *increases* considerably with increasing membrane depolarizations (Figs. 3*D* and 15). The increase of τ_h appears to be correlated with the decrease of the amplitude of the current, as would be expected if the rate of inactivation of h.v.a. channels was directly proportional to the entry of Ca^{2+} ions into the cell. (ii) In the presence of 1 mM-Ba^{2+}, h.v.a. currents were less inactivated than in solutions containing only Ca^{2+}. (iii) The larger the h.v.a. current, the more pronounced, usually, was the inactivation time course (see for example the h.v.a. currents in the middle of Fig. 9).

These findings also suggest that the presence of 10 mM-EGTA at pH 7·2 inside the cell, as in our case, is insufficient to buffer the level of free Ca^{2+} in the vicinity of the membrane (see Byerly & Moody, 1984). This also agrees with the conclusions of Marty

& Neher (1985) from Ca^{2+} currents of chromaffin cells, in which satisfactory Ca^{2+} buffering required the use of higher EGTA concentrations (64 mM at pH 8·2) and thus a buffering capacity about 100 times larger than that in the present study.

Separation of l.v.a. currents

The different sensitivity of l.v.a. and h.v.a. channels to various substances is now well documented. In sensory neurones, l.v.a. but not h.v.a. channels are largely insensitive to various dihydropyridine derivatives (Boll & Lux, 1985; Fedulova *et al.* 1985) as well as to low doses of Cd^{2+} (Nowycky *et al.* 1985; Bossu *et al.* 1985). In heart cells, l.v.a. channels are very little affected by nitrendipine (Bean, 1985). On the other hand, in sensory neurones other compounds such as dopamine (Marchetti, Carbone & Lux, 1986) and menthol (Swandulla, Carbone, Schäfer & Lux, 1987) produce a block of l.v.a. channels and modulate the activation–inactivation kinetics of h.v.a. channels. Dopamine produces a 2- to 10-fold reduction of the activation rate of h.v.a. channels (Marchetti *et al.* 1986), while menthol markedly speeds up the inactivation of h.v.a. channels (Swandulla, Schäfer & Lux, 1986). Our finding that l.v.a. channels persist in the presence of intracellular Ca^{2+} and F^- ions provides an addition to the list of substances with different effects on the two Ca^{2+} channels.

The loss of h.v.a. channels during internal perfusion with high intracellular Ca^{2+} and F^- agrees with previous reports on molluscan (Kostyuk, Krishtal & Shakhovalov, 1977; Kostyuk & Krishtal, 1977) and different vertebrate sensory neurones (Bossu *et al.* 1985; Carbone & Lux, 1985). Discrepancies exist mainly in the critical concentration of intracellular Ca^{2+} needed for complete removal of h.v.a. channels. Kostyuk *et al.* (1977) reported that in *Helix* and *Limnea* neurones a free-Ca^{2+} concentration of about 600 μM was sufficient to produce a rapid disappearance of the classical Ca^{2+} current. Bossu *et al.* (1985) show that in rat cranial neurones the Ca^{2+} concentration required is 10^{-7} M, while in our case (Fig. 13) complete removal of h.v.a. channels occurs at 6 μM using comparable quantities of Ca–EGTA buffers. In our view, such discrepancies are not crucial and are likely to depend on various factors in perfusion techniques and cell types.

A method of separating l.v.a. from h.v.a. channels is simply to dialyse the cell long enough using appropriate salt solutions. This general observation suggests that the two channels have different requirements for survival. As reported in various neurones (Kostyuk, Veselovsky & Fedulova, 1981; Fenwick *et al.* 1982; Dubinsky & Oxford, 1984), h.v.a. channels subside very quickly during cell perfusion with saline solutions. Intracellular applications of cyclic AMP, ATP and Mg^{2+} counteract the run-down of these channels, suggesting that functional states of the h.v.a. channel are preserved by metabolic factors (Fedulova *et al.* 1985).

L.v.a. channels in other preparations

L.v.a. currents of the type described here have been reported to exist in a number of other cell preparations. A Ca^{2+} conductance of the l.v.a. type was first postulated by Llinás & Yarom (1981) to control the firing behaviour of neurones in *in vitro* preparations of the inferior olive, the thalamus (Linás & Jahnsen, 1982) and the dorsal horn (Murase & Randic, 1983). Clonal lines and primary cultures of rat pituitary cells (Armstrong & Matteson, 1985; DeRiemer & Sakmann, 1986),

hypothalamic neurones (Carbone & Lux, 1986*b*), retinal ganglion cells (Grantyn, Johnson & Lux, 1986), hippocampal neurones (Yaari, Hamon & Lux, 1986) and mouse neuroblastoma hybrid cells (Bodewei, Hering, Schubert & Wollenberger, 1985) have been shown to possess Ca^{2+} currents with kinetic and selectivity properties similar to those described here. Recently, an l.v.a. Ca^{2+} current sensitive to holding potential, carried by Ca^{2+} and Ba^{2+} ions, has also been reported in heart cells (Bean, 1985; Nilius, Hess, Lansman & Tsien, 1985; Mitra & Morad, 1986), twitch muscle fibres (Cota & Stefani, 1986), rat myoballs (Cognard, Lazdunski & Romey, 1986) and in vascular smooth muscle cells (Sturek & Hermsmeyer, 1986).

An l.v.a. Ca^{2+} current with similar characteristics but dependent on external NaCl was first observed in the eggs of a starfish (Hagiwara, Ozawa & Sand, 1975). Inactivation was voltage dependent and considerably faster than that of the classical Ca^{2+} channel. Also, polychaete eggs (Fox, 1981; Fox & Krasne, 1984), the ciliate *Stylonichia* (Deitmer, 1984) and mouse neoplastic B lymphocytes (Fukushima & Hagiwara, 1985) show Ca^{2+} currents closely resembling l.v.a. currents. In eggs (Hagiwara *et al.* 1975; Fox & Krasne, 1984), rat d.r.g. cells (Carbone & Lux, 1986*b*) and rat pituitary cells (DeRiemer & Sakmann, 1986), the current carried by these channels is comparable to or is even larger than that through the high-threshold channels. Thus, besides generating and pace-making spikes, the l.v.a. channel may be involved in the control near resting potential of some intracellular Ca^{2+}-dependent processes.

Other Ca^{2+} currents

It has recently been observed that in avian sensory neurones some h.v.a. currents inactivate more completely than others. Inactivation of these currents was attributed to the existence of a third type of Ca^{2+} channel which activates transiently positive to +10 mV and is fully deactivated below −50 mV (Nowycky *et al.* 1985). In our case, about one-tenth of the cells revealed h.v.a. currents with similarly prominent inactivation. Indeed, these samples consisted of neurones having either unusually large l.v.a. currents or incompletely blocked outward K^+ currents. Strongly inactivated and large (−1 to −2 nA) h.v.a. currents were also observed in well-perfused cells. In this case, however, we could not exclude the possibility that, despite Ca buffering, inactivation was fostered by the entry of Ca^{2+} into the cell.

Although our present data on vertebrate sensory neurones do not corroborate conclusions in favour of a third type of Ca^{2+} current, we cannot exclude that sub-populations of d.r.g. cells or other types of cells might possess this current. However, a clear separation of it from the classical high-threshold Ca^{2+} current may necessitate specific pharmacological tools to eliminate either one of these currents.

We are grateful to Drs Arthur Konnerth, Martin Morad and Dieter Swandulla for valuable discussions and criticisms of the manuscript. We thank also Mrs Irene Kiss and Helma Tyrlas for excellent technical assistance, and Mrs Sigrid Messerschmidt for help in preparing the manuscript.

REFERENCES

AKAIKE, N., LEE, K. S. & BROWN, A. M. (1978). The calcium current of *Helix* neuron. *Journal of General Physiology* **71**, 509–531.

ARMSTRONG, C. M. & MATTESON, D. R. (1985). Two distinct populations of calcium channels in a clonal line of pituitary cells. *Science* **227**, 65–67.

BARDE, Y. A., EDGAR, D. & THOENEN, H. (1980). Sensory neurons in culture: changing requirements of survival factors during embryonic development. *Proceedings of the National Academy of Sciences of the U.S.A.* **77**, 199–203.

BEAN, B. P. (1985). Two kinds of calcium channels in canine atrial cells. *Journal of General Physiology* **86**, 1–31.

BJERRUM, J., SCHWARZENBACH, G. & SILLEN, L. G. (1957). *Stability Constants*, part I: *Organic Ligands*. London: The Chemical Society.

BODEWEI, R., HERING, S., SCHUBERT, B. & WOLLENBERGER, A. (1985). Sodium and calcium currents in neuroblastoma and glioma cells before and after morphological differentiation by dibutyryl cyclic AMP. *General Physiology and Biophysics* **4**, 113–127.

BOLL, W. & LUX, H. D. (1985). Action of organic antagonists on neuronal calcium currents. *Neuroscience Letters* **56**, 335–339.

BOSSU, J. L., FELTZ, A. & THOMANN, J. M. (1985). Depolarization elicits two distinct calcium currents in vertebrate sensory neurons. *Pflügers Archiv* **403**, 360–368.

BYERLY, L. & MOODY, W. J. (1984). Intracellular calcium ions and calcium currents in perfused neurones of the snail, *Lymnaea stagnalis*. *Journal of Physiology* **352**, 637–652.

CARBONE, E. & LUX, H. D. (1984*a*). A low voltage-activated calcium conductance in embryonic chick sensory neurons. *Biophysical Journal* **46**, 413–418.

CARBONE, E. & LUX, H. D. (1984*b*). A low voltage-activated, fully inactivating Ca channel in vertebrate sensory neurones. *Nature* **310**, 501–502.

CARBONE, E. & LUX, H. D. (1985). Isolation of low-threshold Ca^{2+} currents in vertebrate sensory neurons. *Pflügers Archiv* **405**, R39.

CARBONE, E. & LUX, H. D. (1986*a*). Sodium channels in cultured chick dorsal root ganglion neurons. *European Biophysical Journal* **13**, 259–271.

CARBONE, E. & LUX, H. D. (1986*b*). Low and high voltage-activated Ca^{2+} channels in vertebrate cultured neurons: properties and functions. In *Calcium Electrogenesis and Neuronal Functioning*, ed. HEINEMANN, U., KLEE, M., NEHER, E. & SINGER, W., pp. 1–8. Heidelberg: Springer Verlag.

COGNARD, C., LAZDUNSKI, M. & ROMEY, G. (1986). Different types of Ca^{2+} channels in mammalian skeletal muscle cells in culture. *Proceedings of the National Academy of Sciences of the U.S.A.* **83**, 517–521.

COTA, G. & STEFANI, E. (1986). A fast-activated inward Ca^{2+} current in twitch muscle fibres of the frog *Rana montezume*. *Journal of Physiology* **370**, 151–163.

DEITMER, J. W. (1984). Evidence for two voltage-dependent calcium currents in the membrane of the ciliata *Stylonychia*. *Journal of Physiology* **355**, 137–159.

DERIEMER, S. A. & SAKMANN, B. (1986). Two calcium currents in normal rat anterior pituitary cells identified by a plaque assay. In *Calcium Electrogenesis and Neuronal Functioning*, ed. HEINEMANN, U., KLEE, M., NEHER, E. & SINGER, W., pp. 139–154. Heidelberg: Springer Verlag.

DUBINSKY, I. M. & OXFORD, G. S. (1984). Ionic currents in two strains of rat anterior pituitary tumor cells. *Journal of General Physiology* **83**, 309–339.

ECKERT, R. & CHAD, J. E. (1984). Inactivation of Ca^{2+} channels. *Progress in Biophysics and Molecular Biology* **44**, 215–267.

FEDULOVA, S. A., KOSTYUK, P. G. & VESELOVSKY, N. S. (1985). Two types of calcium channels in the somatic membrane of new-born rat dorsal root ganglion neurones. *Journal of Physiology* **359**, 431–446.

FENWICK, E. M., MARTY, A. & NEHER, E. (1982). Sodium and calcium channels in bovine chromaffin cells. *Journal of Physiology* **331**, 599–635.

FOX, A. P. (1981). Voltage-dependent inactivation of a calcium channel. *Proceedings of the National Academy of Sciences of the U.S.A.* **78**, 953–956.

FOX, A. P. & KRASNE, S. (1984). Two calcium currents in *Neanthes arenaceodentatus* egg cell membranes. *Journal of Physiology* **356**, 491–505.

FUKUSHIMA, Y. & HAGIWARA, S. (1985). Currents carried by monovalent cations through calcium channels in mouse neoplastic B lymphocytes. *Journal of Physiology* **358**, 255–284.

GRANTYN, R., JOHNSON, J. & LUX, H. D. (1986). Inward currents of rat retinal ganglion cells in dissociated cell culture. *Neuroscience Letters Supplement* **26**, 243.

HAGIWARA, S. & BYERLY, L. (1981). Calcium channels. *Annual Review of Neuroscience* **4**, 69–125.

HAGIWARA, S., OZAWA, S. & SAND, O. (1975). Voltage clamp analysis of two inward current mechanisms in the egg cell membrane of a starfish. *Journal of General Physiology* **65**, 617–644.

HAMILL, O. P., MARTY, A., NEHER, E., SAKMANN, B. & SIGWORTH, F. J. (1981). Improved patch-clamp techniques for high-resolution current recording from cells and cell-free membrane patches. *Pflügers Archiv* **391**, 85–100.

KOSTYUK, P. G. & KRISHTAL, O. A. (1977). Effects of calcium-chelating agents on the inward and outward current in the membrane of mollusc neurones. *Journal of Physiology* **270**, 569–580.

KOSTYUK, P. G., KRISHTAL, O. A. & SHAKHOVALOV, Y. A. (1977). Separation of sodium and calcium currents in the somatic membrane of mollusc neurones. *Journal of Physiology* **270**, 545–568.

KOSTYUK, P. G., VESELOVSKY, N. S. & FEDULOVA, S. A. (1981). Ionic currents in the somatic membrane of rat dorsal root ganglion neurons – II. Calcium currents. *Neuroscience* **6**, 2431–2437.

LLINÁS, R. & JAHNSEN, H. (1982). Electrophysiology of mammalian thalamic neurones *in vitro*. *Nature* **297**, 406–408.

LLINÁS, R. & YAROM, Y. (1981). Properties and distribution of ionic conductances generating electroresponsiveness of mammalian inferior olivary neurons *in vitro*. *Journal of Physiology* **315**, 569–584.

LUX, H. D. & BROWN, A. M. (1984). Patch and whole cell calcium currents recorded simultaneously in snail neurons. *Journal of General Physiology* **83**, 727–750.

MACKIE, G. O. & MEECH, R. W. (1985). Separate sodium and calcium spikes in the same axon. *Nature* **313**, 791–793.

MARCHETTI, C., CARBONE, E. & LUX, H. D. (1986). Effects of dopamine and noradrenaline on Ca^{2+} channels of cultured sensory and sympathetic neurons of chick. *Pflügers Archiv* **406**, 104–111.

MARTELL, A. E. & SMITH, R. M. (1974). *Critical Stability Constants*, vol. 1: *Amino Acids*. New York: Plenum Press.

MARTY, A. & NEHER, E. (1985). Potassium channels in bovine adrenal chromaffin cells. *Journal of Physiology* **367**, 117–141.

MATTESON, D. R. & ARMSTRONG, C. M. (1986). Properties of two types of calcium channels in clonal pituitary cells. *Journal of General Physiology* **87**, 161–182.

MITRA, R. & MORAD, M. (1986). Two calcium channels in guinea pig ventricular myocytes. *Proceedings of the National Academy of Sciences of the U.S.A.* (in the Press).

MURASE, K. & RANDIC, M. (1983). Electrophysiological properties of rat spinal dorsal horn neurones *in vitro*: calcium-dependent action potentials. *Journal of Physiology* **334**, 141–153.

NILIUS, B., HESS, P., LANSMAN, J. B. & TSIEN, R. W. (1985). A novel type of cardiac calcium channel in ventricular cells. *Nature* **316**, 443–446.

NOWYCKY, M. C., FOX, A. P. & TSIEN, R. W. (1985). Three types of neuronal calcium channels with different agonist sensitivity. *Nature* **316**, 440–443.

STUREK, M. & HERMSMEYER, K. (1986). Two different types of calcium channels in spontaneously contracting vascular smooth muscle cells. *Journal of General Physiology* **86**, 23a.

SWANDULLA, D., CARBONE, E., SCHÄFER, K. & LUX, H. D. (1987). Effect of menthol on two types of Ca currents in cultured sensory neurons of vertebrate. *Pflügers Archiv* (in the Press).

SWANDULLA, D., SCHÄFER, K. & LUX, H. D. (1986). Ca^{2+} channel current inactivation is selectively modulated by menthol. *Neuroscience Letters* **68**, 23–28.

YAARI, Y., HAMON, B. & LUX, H. D. (1986). Two types of calcium conductances in cultured mammalian hippocampal neurons. *Society for Neuroscience Abstracts* **12**, 1347.